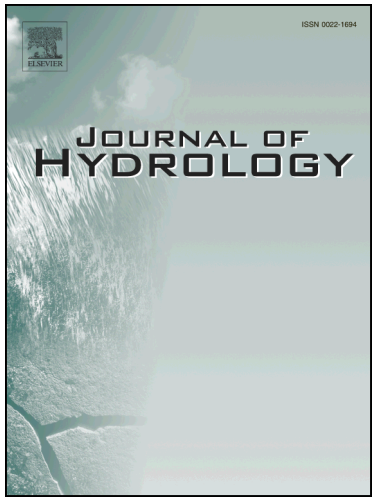

Research papers

Controls on dripwater chemistry of Oregon Caves National Monument, northwestern United States

Ahmed I. Rushdi, Vasile Ersek, Alan C. Mix, Peter U. Clark

PII: S0022-1694(17)30824-7
DOI: https://doi.org/10.1016/j.jhydrol.2017.12.006
Reference: HYDROL 22417

To appear in: *Journal of Hydrology*

Received Date: 11 July 2017
Accepted Date: 3 December 2017

Please cite this article as: Rushdi, A.I., Ersek, V., Mix, A.C., Clark, P.U., Controls on dripwater chemistry of Oregon Caves National Monument, northwestern United States, *Journal of Hydrology* (2017), doi: https://doi.org/10.1016/j.jhydrol.2017.12.006

To: Journal of Hydrology

Controls on dripwater chemistry of Oregon Caves National Monument, northwestern United States

Ahmed I. Rushdi[1,*], Vasile Ersek[2], Alan C. Mix[3], Peter U. Clark[3]

[1] ETAL, 2951 SE Midvale Dr., Corvallis OR 97333, U.S.A.

[2] Department of Geography, Northumbria University, NE1 8ST UK

[3] College of Earth, Oceanic and Atmospheric Sciences, Oregon State University, Corvallis OR 97331, U.S.A.

[*] Corresponding author: arushdi@ksu.edu.sa or airushdi@comast.net

Abstract

Cave dripwater chemistry of Oregon Caves National Monument (OCNM) was studied, where the parameters pH, total alkalinity, calcium, magnesium, strontium, sodium and barium were analyzed at quasi-monthly intervals from 2005 to 2007. Different statistical analyses have been used to investigate the variability of the chemical parameters in the different sites in the OCNM cave system. The dripwater varies in response to seasonal changes in rainfall. The drip rates range from zero in summer to continuous flow in winter, closely following the rainfall intensity. Spatial variations of dripwater chemistry, which is nonlinearly related to dripwater discharge likely, reflect the chemical composition of bedrock and overlying soil, and the residence time of the ground water within the aquifer. The residence time of infiltrated water in bedrock cracks control the dissolution carbonate bedrock, reprecipitation of calcium carbonate and the degree of saturation of dripwater with respect to calcium carbonate minerals. Spatiotemporal fluctuations of dripwater Mg/Ca and Sr/Ca ratios are controlled by dissolution of carbonate bedrock and the degree of calcite reprecipitation in bedrock cracks. This suggests that trace elements in speleothem deposits at the OCNM may serve as paleoclimatological proxies for precipitation, if interpreted within the context of understanding local bedrock chemistry.

Keywords: OCNM, Oregon, speleothem, geochemistry, dripwater, Mg/Ca, Sr/Ca

1. Introduction

Interactions between rain, soil, and bedrock produce a variety of biogeochemical signals in cave dripwaters including $\delta^{18}O$ and δD from rain, traces of organic matter, $\delta^{13}C$ of total dissolved CO_2 and elements such as calcium, magnesium, strontium. Dripwater properties depend on the surrounding environmental conditions and on the dissolution and precipitation processes in the karst system (Fairchild et al., 2000; 2006; Toran and Roman, 2006; Borsato et al., 2015; Casteel and Banner, 2015; Zeng et al., 2015). Studies of limestone caves identified seasonal variations in ionic concentrations of dripwaters (Baker et al., 2000; Drever, 1982; Musgrove and Banner, 2004; Day and Henderson, 2013). For example, total dissolved ion concentrations in dripwaters were observed to correlate with soil CO_2 seasonal variations (Mayer, 1999) because higher levels of soil CO_2 increase carbonate mineral dissolution. The composition of the host rock also strongly influences the water composition (Motyka et al., 2005; Smart et al., 1986; Tooth and Fairchild, 2003). Dripwaters with high concentrations of calcium and bicarbonate are mainly produced from calcitic bedrock while waters with high concentrations of calcium, magnesium, bicarbonate, and sulfate are produced from dolomitic bedrock with pyrite (Chalmin et al., 2007; Bar-Matthews et al., 1991; Frisia et al., 2002; Wu et al., 2015). The variation in physical and chemical properties of dripwater may be incorporated and preserved in speleothem deposits, and these changes have been used to infer paleoclimate and paleoenvironmental conditions in the caves where speleothem deposits were formed (McDermott, 2004; Fairchild et al., 2006; Johnson et al., 2006; McDonald et al., 2007; Lachniet 2009, Steponaitis et al., 2015). The physicochemical characteristics of the drip waters can help in understanding the processes that affect the formation of stalagmites

and carbon, hydrogen and oxygen isotopic composition (McDonald et al., 2007; Lambert and Aharon, 2011).

Drip water rates change seasonally and vary from slow and irregular to fast and continuous (Baker and Brunsdon, 2003; Baker et al., 2000; Fernández-Cortés et al., 2007). The drip water rates in the Oregon Caves National Monumnent (OCNM) also vary seasonally and range from slow to no drip at shallow rooms to fast and constant drip at the deeper rooms (Schubert 2007). The control of drip water rate and room locality (i.e, shallow vs depth) on the drip water chemistry has not been fully investigated. Therefore, the objectives of this work were to: (1) characterize the geochemistry and the saturation states of the waters with respect to carbonate minerals and (2) investigate the possible factors that control dripwater chemistry and their potential influence on the chemical composition of speleothems from shallow (slow dripwater rate) and deep (fast dripwater rate) rooms. Here, we analyze dripwaters from the OCNM in southwestern Oregon of the USA.

2. Study Area and Sampling Sites

The OCNM is located in the Klamath Mountains, southwestern Oregon (42^{o} 05' 53" N, 123^{o} 24' 26" W, altitude ~1220m) (Fig. 1). The modern vegetation above the cave is dominated by *Pseudotsuga menziesii* (Douglas fir) and *Abies concolor* (white fir). The plants are mainly of C-3 type vegetation. Soils overlying the OCNM are from various bedrock lithologies including granites and serpentinites. The bedrock in the OCNM cave system belongs to the Paleozoic-Triassic Applegate Group, consisting of metavolcanics and metasediments (Irwin, 1966; Barnes et al., 1996). The OCNM was formed in a

faulted and folded marble lens, and was carved by meteoric waters that have percolated through the overlying soil and bedrock (Barnes et al., 1996; Vacco et al., 2005; Schubert, 2007).

The measured temperature deep inside the cave is approximately constant through the year at 8.8±0.7°C. The monthly-average temperature outside the cave ranges from ~19°C in summer to ~6.5°C in winter (Schubert, 2007). Precipitation falls mostly as rain in the fall and spring and as snow in winter, but is virtually absent in summer (Taylor and Hannan, 1999). Water entering the cave is derived from local snowmelt and rainfall (Ersek et al., 2010). Rainfall events activate dripwater sites within hours to days in the upper part of the cave, although water also may take months to years to reach the cave through cracks parallel to the orientation of the bedrock structure (Roth, 2005). While upper parts of the cave dry out by the end of summer, deeper parts remain wet throughout the year (Schubert, 2007).

3. Methodology

3.1. Sampling

Dripwater samples were collected at four sites within the OCNM cave system (Fig. 1) at quasi-monthly intervals from January, 2005 to July, 2007. We collected the water samples manually and used a stopwatch to count the number of drips/minute. We did this 3 times and averaged the number. Precipitation data were obtained from a weather station installed outside the cave. Collection sites were situated in the the Kings and Queens Throne Room (KQR, ~14 meters subsurface), Imagination Room (IR, ~18 m subsurface), the Miller's Chapel Room (MR, ~30 m subsurface), and from two sites in

the Shower Room (SR1 and SR2, ~51 m subsurface). All water samples were collected into dark amber glass bottles with airtight screw-cap seals and plastic vapor barriers which were acid-washed, rinsed with deionized water purified with Milli-Q Plus Water System (Millipore) prior to use. Nitric acid was added to each sample to achieve pH ~ 1.0 (Cenci and Martin, 2004).

. The samples were subsequently stored in a refrigerator for 1-12 months before analysis, where the pH and total alkalinity measurements were performed during the first 2-3 months of the sample collection. The analyses of trace and major elements were conducted 3-6 months later.

3.2. Chemical Analyses

The bottles were carefully sealed to ensure that they remain gas-tight to prevent any atmospheric gas exchange. We divided the water samples into two aliquots. The first aliquot, which was drawn slowly from the top 5 cm of the solution, was used for pH and total alkalinity measurements, and the second aliquot was used for isotopic (Ersek et al., 2010) and major and minor element analyses. As sample pH can be affected by gas exchange, the pH and total alkalinity measurements were performed in closed cell to avoid any opportunity to CO_2 exchange with atmosphere.

pH Benchtop meter (Thermo Scientific™ Orion Star™ A211) was used to measure pH and total alkalinity. Before proceeding with any pH and titration measurements, we standardized the electrodes in two VWR buffer solutions assigned pH of 4.63 ± 0.02 at $25^{o}C$ (4.62 ± 0.02 at $20^{o}C$) and pH of 7.38 ± 0.02 at $25^{o}C$ (7.39 ± 0.02 at $20^{o}C$), and determined the slope, S, of the electrode, expressed in mv/pH. We compared

the slope with the theoretical one (e.g., S = 58.178 mv/pH at 20°C) and if measurements were within 1%, the theoretical value was usually used. The practical slope for six different measurements had a standard deviation of ±0.099 mv/pH and % error ranged from -0.325 to 0.117%. The measured pH, pH_m, was calculated from:

$$pH_m = pH_b + \frac{E_m - E_b}{S} \qquad (1)$$

where pH_b is the pH of the standard buffer solution, and E_m and E_b are the electrode potential in the test solution and in the standard buffer, respectively. No significant drift in pH electrode was observed during the routine measurements. The reproducibility of the pH measurements was found to range from 0.009-0.024pH unit at pH > 7.50 and from 0.005-0.013pH unit for pH < 4.00.

Total alkalinity (TA) of each test solution was measured using the Gran titration method (Gran, 1952; Dyrssen and Sillen, 1967; Mehrbach et al, 1973; Rushdi et al., 1998). The standard deviation of total alkalinity was ±5.8 μeq L^{-1} solution.

We analyzed major and trace metals by inductive coupled plasma-mass spectrometry at the W.M. Keck Collaboratory, College of Oceanic and Atmospheric Sciences, Oregon State University. The metals (and their detection limits) included calcium (Ca) (0.1 ppm), magnesium (Mg) (0.4 ppb), strontium (Sr) (0.1 ppb), barium (Ba) (0.1 ppb), and sodium (Na) (3 ppb). Deionized water was used to prepare the calibration and quality control solutions. Nitric acid was added to the matrix of the standard and quality control solutions to achieve pH ~ 1.0. We analyzed reference solutions every 10-20 samples to monitor the stability of analytical system. Standard deviations of triplicate

159 analyses were better than <5%. The concentrations of potassium (K^+), chlorine (Cl^-) and
160 sulfate (SO_4^{2+}) ions were obtained from the data of a different project, studying the
161 dripwater chemistry of same rooms, by Schubert (2007).
162
163 3.3. Degree of saturation with respect to carbonate minerals
164 The saturation states of the solutions are calculated at in situ temperatures using
165 the ratio of ionic products (IP) to solubility constants (K_{sp}) of the mineral of interest (i.e.,
166 IP/Ksp). This value is known as degree of saturation (Ω), saturation ratio, and saturation
167 index (SI) (Picknett et al., 1976). The percent degree of saturation (%Ω) with respect to
168 different carbonate minerals was calculated from:
169

$$\%\Omega = \left[\frac{(Ca^{2+})_T * CA \dfrac{K_2}{(\gamma_{H^+})_T (H^+)_T + 2K_2}}{\dfrac{K_{sp}^0}{(\gamma_{Ca^{2+}})_T (\gamma_{CO_3^{2-}})_T}} \right] * 100 \qquad (2)$$

170
171

$$K_2 = \frac{K_2^0 (\gamma_{HCO_3^-})_T}{(\gamma_{H^+})_T (\gamma_{CO_3^{2-}})_T} \qquad (3)$$

172
173
174 where CA is the carbonate alkalinity (CA = (HCO_3^-) + (CO_3^{2-})); $(\gamma_i)_T$ is the total activity
175 coefficient of the species $(i)_T$ (Davies, 1962); and K_2 and K_2^0 are the second
176 stoichiometric and thermodynamic dissociation constants of carbon acid (Hanred and
177 Scholes 1941); K_{sp} and K_{sp}^0 are the stoichiometric and thermodynamic solubility
178 constants of the mineral calcium carbonate, respectively (Plummer and Bunsenberg,

1982). The concentration ranges of Cl^-, K^+ and SO_4^{2-} of the dripwaters (Schurbet, 2007) were small relative to Ca^{2+}, HCO_3^- and CO_3^{2-} and did not affect the computed values of Ca^{2+} and CO_3^{2-} activity coefficients; thus, their concentration effects on the saturation states of calcium carbonate minerals are insignificant.

Values of %Ω were estimated for pure calcite, aragonite, and vaterite minerals. Our calculation was in a good agreement with the values estimated by Schubert (2007) using PHREEQC1 speciation water resource application software (Parkhurst, 200).

3.4. Statistical analysis

The statistical analyses including linear relationships between different physical and chemical parameters, cluster analysis (CA) and principal component analysis (PCA) were performed using the SPSS (IBM-Statistical Package for the Social Sciences, version 16.0).

4. Results and discussion

4.1. Rainfall and Dripwater rates

In 2005, precipitation was up to 25.1 millimeter per month (mm m^{-1}), with maximum rain occurring in October. The amount of precipitation increased in 2006 with a maximum amount in November (276.9 mm m^{-1}) and December (368.3 mm m^{-1}) (Fig. 2). The increase in the amount of precipitation was also significant in 2007, where the maximum rainfall was recorded in October and November (234.4 and 117.9 mm m^{-1}, respectively). The average amount of rainfall increased significantly from 7.4 mm m^{-1} in

2005 (July-December), 70.9 mm m^{-1} in 2006 (January-December) to 92.7 mm m^{-1} in 2007 (January-November).

The amount of water that infiltrates into caves depends on the types of soil and bedrock above the cave, the hydrology of the karst aquifer, and the water source (Atkinon, 1977; Ford and Williams, 1989; Tooth and Fairchild, 2003; McDonald and Drysdale, 2007). The drip rates at the OCNM range from no drip to continuous discharge at all sites except SR1 and SR2, where water flows throughout the year, and increase with the increase of the rainfall outside the cave (Fig. 2). At the other sites, there was no water discharge during much of the summer. After times of low or no rainfall, the water discharge in the cave usually starts a month after precipitation events. After heavy rainfall events the drip rates typically increases within 3-7 days. The drip rates were highest at the deepest sites (SR2 and SR1) and lowest at the shallowest site (IR) (Fig. 2b) but were not monotonically related to depth in the cave (KQR> MR).

4.2. Chemical parameters and dripwater rates

The chemical analyses of the dripwater samples (pH, total alkalinity, calcium, magnesium, strontium, barium and sodium) are shown Figure 2. Obviously, the major and trace metal concentrations varied both seasonally and spatially (Fig. 2) where the highest concentrations were observed between November and December and deeper rooms with discrete drippings. For the purpose of understanding the similarity and dissimilarity among the different sites, the data set was statistically analyzed by cluster analysis; it was performed with the standardized data by Z score using Ward's method with squared Euclidean distances. The cluster analysis of the chemical parameters (Figure

3a) shows that only two groups were recognized; the first group included IR and KQR (< 18 m depth) and the second group included MR, SR1 and SR2 (> 30 m depth). The depth of the site from surface and dripwater discharge also appears to affect calcium variability. Sites in the cave that are shallower (IR, KQR) or have slow drip rates (MR) show higher Ca^{2+} and Mg^{2+} variability than deep cave sites (SR1 and SR2). Slightly higher concentrations of calcium and magnesium are also detected when water discharges are slow at deeper drip sites.

The levels of the various measured parameters have been submitted to simple regression analyses to examine any probable correlation among them with emphasis on the dripwater rates for shallow and deep rooms. The correlations between the different physicochemical parameters of the shallow and deep rooms are shown in Table 1. For the shallower (<18m depth) site rooms such as the QKR and IR, the significant correlations are mainly for TA-Ca^{2+} and Mg^{2+}-Sr^{2+} ($p < 0.01$), where the dripwater rates are slow. The lack of significant correlations between other parameters such as TA-Mg^{2+}, TA-Sr^{2+}, Mg^{2+}-Ca^{2+}, Ca^{2+}-Sr^{2+} is possibly due to incongruent dissolution and re-precipitation of calcium carbonate of different carbonate minerals. In deeper rooms (> 30 m depth) such as MR, SR1 and SR2, where the dripwater rates are discrete, the correlations are significant for Drip-pH, pH-Sr^{2+}, TA-Ca^{2+}, TA-Ca^{2+} and Mg^{2+}-Sr^{2+} likely is caused mainly by congruent dissolution of carbonate bed rock. Obviously, dissolution process is the limiting factor that controls the concentrations of elements when the drip rates are continuous and fast. This indicates that residence time of percolated water in epikarst likely influences the concentration of elements in dripwaters.

Storage capacity and orientation of bedrock fractures influence the concentrations of major and trace elements in dripwaters (Tooth and Fairchild, 2003). Slow-moving ground waters require recharge threshold to reach different parts of the cave system. The major change in the water composition around November 2005 and 2006 is consistent with the increase in rainfall prior to these periods (September, 2005 and October, 2006). These concentration peaks are followed by decreases in these chemical parameters a month after November that persist throughout the rest of the rainy season.

4.3. Processes controlling dripwater chemistry

Because of relatively high pCO_2 derived from plant respiration and organic matter decay, dissolution processes are the main reactions in both the soil and epikarst zones (Hindy, 1971; Mayer, 1999). Therefore, dripwater solutions have geochemical information from rainfall, the soil component including organic matter and elements such as calcium, magnesium, strontium and phosphorous, and the mineralogy of the epikarst zone where dissolution and reprecipitation of calcium, magnesium, and strontium are expected.

To determine the possible sources of elements and physical and chemical processes that control the concentrations of the measured parameters, principle component analysis (PCA) was performed with the correlation coefficient matrix and the variance rotation with Kaiser Normalization. PCA analysis, with eigen value > 1.0, identified two principle components for shallow and deeper rooms (Table 2). Factor loadings of > 0.75 for variables were used for interpretation.

By treating the karst as one homogenous system and using all the data set to predict PC factors to physicochemical parameters, two principle components were extracted explaining 91.96% of the total variance. PC1 explains 78.62% of the variance, with pH, TA, Ba^{2+}, Ca^{2+}, Mg^{2+} and Na^{+} as the predominant parameters (Fig. 3b). Thus, PC1 represents the major processes controlling the dripwater components, which are mainly dissolution of the bed rock, solid-solution reaction and water-rock ion exchange. A 13.34% of the variance is explained by PC2 showing a significant factor loading for Sr^{2+}, likely dissolution of minerals containing strontium (e.g., crawfordite ($Na_3Sr(PO_4)(CO_3)$), strontianite ($SrCO_3$) and celestite ($SrSO_3$)).

The relationship between calcium and other elements can be used to investigate the dominant reactions and sources of these elements (Fairchild et al., 2000; McDonald et al., 2007; Cruz et al., 2007; Karmann et al., 2007). Table 2 shows the correlation between various elements and calcium concentrations in dripwater solutions. Both magnesium and strontium concentrations show significant positive correlations with calcium concentrations (Table 2) at the IR, SR1 and SR2 sites. This suggests that the main source of these elements (i.e., calcium, magnesium and strontium) is the dissolution of carbonate minerals in bedrock, which also confirmed by the results of PCA. These correlations are insignificant in the KQR and MR dripwater sites suggesting that the dissolution/re-precipitation reactions of carbonate minerals might not be the main sources of the major elements (i.e., Ca, Mg and Sr) in the solutions of these dripwater sites. Another explanation for this lower correlation is the dissolution of other minerals beside carbonate minerals such as calcium sulfate ($CaSO_{4(s)}$). Sodium and barium show poor correlations

with calcium (Table 2), which suggest that the main source of these elements is the soil cover.

Since the dissolution and/or the precipitation of calcium carbonate ($CaCO_{3(s)}$) affects both total carbon dioxide and total alkalinity, the contribution of $CaCO_{3(s)}$ can be confirmed by the correlation between TA calcium ion (Ca^{2+}) concentrations. The correlations between TA and Ca^{2+} is significant at shallow and deep sites (r = 0.82-0.92) (Table 1), indicating that $CaCO_{3(s)}$ is the major source of calcium ions. The number of moles of CO_3^{2-} that are involved in the formation of $CaCO_{3(s)}$ or are released as a result of $CaCO_{3(s)}$ dissolution will change the carbonate alkalinity by a factor of 2 according to equation ($CA = (HCO_3^-) + 2(CO_3^{2-})$). Thus, one would expect to obtain a slope of 2 by plotting CA against Ca^{2+} if the main cause of the CA change is the dissolution or precipitation of $CaCO_{3(s)}$. The estimated slopes are respectively 1.91, 1.98 and 1.96 and 1.67 (1.88 ± 0.14) for the IR, MR, SR1 and SR2 sites (Fig. 4b), confirming that $CaCO_{3(s)}$ bedrock is the main source of Ca, Mg, and Sr in IR, MR and SR sites. This is also supported by the significant correlations between Mg-Ca and Sr-Ca for SR1 and SR2 (Table 2). The slope of 1.07 for the KQR site suggests that additional minerals are involved in the contribution of Ca concentration in dripwater. One of these minerals is likely to be $CaSO_{4(s)}$, which will increase the concentration of calcium ion relative to carbonate alkalinity and eventually reduce the slope.

4.4. The saturation levels of dripwater solutions with respect to carbonate minerals

Values of %Ω were estimated for pure calcite, aragonite, and vaterite minerals. All sites showed that the dripwaters were supersaturated with respect to pure calcite and

aragonite and undersaturated with respect to vaterite (Table 4; Fig. 5). They ranged from 86% to 528% (mean = 262±111), 59% to 368% (mean = 182±77), and 21% to 128% (mean = 63±26) for calcite, aragonite and vaterite, respectively.

The degree of saturation of the dripwater is an important parameter to assess its chemistry and the tendency for stalagmite formation or dissolution. At the KQR and MR sites, the dripwaters were saturated to supersaturated with respect to pure calcite and aragonite and undersatruated to supersaturated at IR SR1 and SR2 sites. All sites are undersaturated to saturated with respect to vaterite. We also note that the degree of saturation generally increases with the decreases of drip rates in May-June 2006 and 2007, when solutions become more supersaturated when the drip rate is slow (Figs 2 and 5).

Various natural waters (i.e., spring, ground, oceanic and pore waters) are often found to be supersaturated with respect to both calcite and aragonite, but without inorganic precipitation of $CaCO_{3(s)}$ (Weyle, 1961; Pytkowicz, 1965; Berner, 1975). It is well established that the magnesium content of calcite has a direct effect on the physical and chemical behavior of $CaCO_{3(s)}$ and its solubility (Chave et al., 1962; Bischoff and Fyfe, 1968; Lahann, 1978a,b; Mackenzie et al., 1982; Mucci and Morse, 1984; Mucci et al., 1985; Rushdi, 1995; Rushdi et al., 1992, 1998). Chave et al.. (1962) showed that the solubility of calcium carbonate increases in the order of pure calcite, low magnesian calcite, aragonite and high magnesian calcite. Previous studies have shown that the solubility of magnesian calcite increases by the increase of Mg content of $CaCO_{3(s)}$ (Plummer and Mckenzie, 1974; Thorstenson and Plummer, 1977; Land, 1967; Chave et al., 1962, Walter and Morse, 1984; Mucci and Morse, 1984; Rushdi et al., 1992, 1998). This may produce dripwater solutions with high Mg concentrations and supersaturated

with respect to pure calcite. The maximum super saturation range where low magnesian calcite may form is about 528% (Rushdi et al., 1998). However, the dripwater solutions are supersaturated with respect to pure calcite and aragonite, so they are likely to be undersaturated with respect to high magensian calcite. Therefore, one would expect that pure and low magnesian calcite will form as a speleothem deposit.

4.5. Mg/Ca and Sr/Ca ratios of dripwaters

Prolonged interaction between groundwater and bedrock enhances dissolution of calcium carbonate bedrock increasing the saturation levels of calcium carbonate and the concentrations of Ca, Mg, Sr and other trace metals in solution. The dripwaters in caves are expected to have a high degree of saturation (i.e., high Ca concentration) (Fig. 6a) with respect to calcium carbonate minerals. Different Mg/Ca and Sr/Ca ratios due to enhanced dissolution of various carbonate minerals and possible calcite reprecipitation are expected (Fairchild et al. 2000; Day and Henderson, 2013). We find that shallow sites show relatively high concentrations of Ca and lower degree of superaturation, whereas deeper sites show lower Ca concentrations and higher degree of super saturation (Fig. 6a). This is likely due to longer contact times of waters and bedrock and reprecipitation of low magnesian calcite in deeper sites.

The Mg/Ca and Sr/Ca ratios fluctuate at slow and fast drip sites (Figs. 2b) and the values of Ca, Mg and Sr concentrations (Fig. 2) also suggest that the bedrock (with different calcium carbonate minerals) is the main factor that influences the chemistry of the dripwaters in the cave. The results also show that there is an increase in the Sr/Ca with the increase of Mg/Ca (Fig. 6b). Shallow sites (e.g. IR) show low values of both

Mg/Ca and Sr/Ca ratios with no obvious trend. This is likely due to reprecipitation of magnesian calcite on the surfaces of bedrock fractures. This is supported by the low Mg/Ca ratios and relatively lower degree of saturation at shallow sites (IR and KQR) relative to the high ratios and higher saturation levels with respect to calcium carbonate in deeper sites (SR1 and SR2) (Fig. 6).

Dilution effects are likely to be insignificant in these dripwater sites; therefore, Ca variation relative to Mg/Ca and Sr/Ca in dripwaters is likely controlled by dissolution of different $CaCO_{3(s)}$ minerals (e.g., calcite with different mole percent Mg, aragonite, and dolomite) and calcite reprecipitation in the routes and cracks above the cave. Calcite reprecipitation apparently increases in dry seasons because air circulation increases in the epikarst as a result of low level of ground waters of high degree of saturation with respect to calcium carbonate (Fairchild et al., 2000; Tooth and Fairchild, 2003; Musgrove and Banner, 2004; McDonald et al., 2004; Fairchild et al., 2006; Day and Henderson, 2013). This will increase the relative co-precipitation of Mg and Sr and decrease the Mg/Ca and Sr/Ca ratios in dripping waters of shallow sites (Fig. 6c and d). During the wet season, when the degree of supersaturation is expected to be comparatively lower, low magnesian calcite precipitates and less Mg and Sr are co-precipitated in the mineral phase leading to high dripwater Mg/Ca and Sr/Ca ratios. Sr/Ca ratios show slightly different behavior due to likely different bedrock carbonate minerals as is explained below.

These observations suggest that the degree of supersaturation of the solution and rate of calcite reprecipitation, which differ seasonally, control the variations of Mg/Ca and Sr/Ca ratios in dripwater solutions. This is because the partition coefficients of Mg and Sr are less than 1 in dilute solutions (Mucci and Morse, 1983; Morse and Bender,

1990; Huang and Fairchild, 2001). In addition, the ionic sizes of Ca (radius = 112 pm), Mg (radius = 86 pm) and Sr (radius = 132 pm) have differing effects on the chemical and physical behaviors of the carbonate minerals. Sr is more commonly associated with aragonite and is found to increase the solubility of aragonite, while Mg is associated with calcite and increases its solubility (Chave et al., 1962; Land, 1967; Plummer and MacKenzie, 1974; Mucci and Morse, 1984; White, 1994, 2004). Usually, the Sr/Ca ratio in aragonite is higher than in calcite, so that the dissolution and transformation of aragonite to calcite releases Sr into the solution (Huang et al., 2001; Fairchid and Killawee, 1995; White, 2004; McMillan et al., 2005). This indicates that the increase in Sr/Ca ratios in KQR is likely attributed to the presence of aragonite in the bedrock.

The exponential decrease of Ca in solution relative to both Mg/Ca and Sr/Ca ratios in these dripwaters (Fig. 6e and f) suggests that calcite reprecipitation, which is clearly shown in shallow sites, can be considered as the key chemical reaction that controls the variation in elemental ratios in dripwater of the OCNM cave system. Therefore, trace metals in speleothem deposits at the OCNM can be used as paleoclimatological proxies for precipitation, if interpreted within the context of understanding local bedrock chemistry.

5. Conclusions and paleoclimate implications

Dissolution and reprecipitation are likely the main processes that control the chemistry of the dripwaters in the OCNM cave system. Calcite reprecipitation could be a key process at parts of the epikarst and causes homogenous short-term variation in major

and trace elements in dripwaters in the system. Seasons with low rainfall are associated with increases in Ca, Mg, and Sr concentrations karst solutions. This is followed by relative increases in Mg/Ca and Sr/Ca concentration ratios relative to the concentration of Ca in the dripwaters due to re-precipitation of calcite along flow routes.

Spatiotemporal covariance of chemical parameter suggests that stalagmites in this cave might record the major and trace metal variations as a result of changes in hydrological conditions. In particular, Mg/Ca and Sr/Ca in speleothems from OCNM may serve as proxies of past climate. The spatial chemical variations in the OCNM cave waters are apparently influenced by the mineralogy of the bedrock and the flow routes, which cause the differences in their values and the slopes of Mg/Ca and Sr/Ca ratio trends. This suggests that Mg/Ca and Sr/Ca at a given location in the ONCM cave system can be used as qualitative proxies for seasonal changes of past rainfall as long as groundwater pathways to each site remain constant, but that quantitative interpretations, or combination of data from multiple sites, would require site-specific calibration.

Acknowledgments

The authors thank the staff at Oregon Cave National Monument for their assistance in sampling water.

References

Atkinson, T. C., (1977), Diffuse flow and conduit flow in limestone terrain in Mendip Hills, Somerset (Great Britain). *Journal of Hydrology* 35, 93–110.

Baker, A., D. Genty, and I.J. Fairchild (2000), Hydrological characterization of stalagmite drip water at Grottee de Villars, Dordogne, by the analysis of inorganic species and luminescent organic matter. *Hydrology and Earth System Sciences* 4, 439-449.

Bar-Matthews, M., A. Matthews, and A. Ayalon (1991). Environmental Controls of Speleothem Mineralogy in a Karstic Dolomitic Terrain (Soreq Cave, Israel). The *Journal of Geology*, 99:189-207.

Barnes, C.G., Donato, M.M., Tomlinson, S.L. (1996), The enigmatic Applegate group of southwestern Oregon: Age correlation and tectonic affiliation. *Oregon Geology* 58, 79-91.

Berner, R. A., (1975), The role of magnesium in the crystal growth of calcite and aragonite from sea water. *Geochim. Cosmochim. Acta* 39, 489–504.

Bischoff, J. L., and W. S. Fyfe (1968), The aragonite-calcite transformation. *Am. J. Sci.* 266, 65-79.

Casteel, R. C., and J. L. Banner (2015), Temperature-driven seasonal calcite growth and drip water trace element variations in a well-ventilated Texas cave: Implications for speleothem paleoclimate studies. *Chemical Geology*, 392, 43-58.

Cenci, R. M., and J. M. Martin (2004). Concentration and fate of trace metals in Mekong River Delta. Sci. Total Environ. 332, 167–182.

448 Chalmin, E. F. d'Orlyé, L. Zinger, L. Charlet, R. A. Geremia, G. Orial, M. Menu, D.
449 Baffier, and I. Reiche (2007), Biotic versus abiotic calcite formation on
450 prehistoric cave paintings: the Arcy-sur-Cure 'Grande Grotte' (Yonne, France)
451 case. *Geological Society, London, Special Publications;* 2007; v. 279; p. 185-197;
452 DOI: 10.1144/SP279.15.
453 Chave, K. E., K. S. Deffeyes, P. K. Weyl, R. M. Garrels, and M. E. Thompson (1962),
454 Observations on the solubility of skeletal carbonate in aqueous solution. *Science*
455 137, 33-34.
456 Cruz Jr., F. W., S. J. Burns, M. Jercinovic, I. D. Karmann, W. D. Sharp, and M. Vuille
457 (2007), Evidence of rainfall variations in Southern Brazil from trace element
458 ratios (Mg/Ca and Sr/Ca) in a Late Pleistocene stalagmite. *Geochimica et*
459 *Cosmochimica Acta* 71, 2250–2263.
460 Davies, C. W. (1962), *Ion Association*. Butterworths, London.
461 Day, C. C., and G. M. Henderson (2013), Controls on trace-element partitioning in cave-
462 analogue calcite. *Geochim. Cosmochim. Acta*., 120: 612-627.
463 Drever, J.I., (1982), *The geochemistry of natural waters:* Englewood Cliffs, Prentice-Hall,
464 INC, 388 p.
465 Dyrssen, D., and L. G. Sillen (1967), Alkalinity and total carbonate in seawater. A plea
466 for –T independent data. *Tellus*, 19, 113-121.
467 Ersek V., A. C. Mix, and P. U. Clark (2010), Variations of $\delta^{18}O$ in rainwater from
468 southwestern Oregon. *J. Geophys. Res.*:D09109, doi:10.1029/2009JD013345
469 Fairchild, I.J., A. Borsato, A. Tooth, S. Frisia, C. J. Hawkesworth, Y. Huang, F.
470 McDermott, and B. Spiro (2000), Controls on trace element (Sr-Mg)

compositions of carbonate cave water: implications for speleothem climatic records. *Chemical Geology* 166, 255-269.

Fairchild, I. J., and J. A. Killawee (1995), Selective leaching in glacierized terrains and implications for retention of primary chemical signals in carbonate rocks. In: Kharaka, Y. K., and O. V._Chudaev, Eds., *Water–Rock Interaction*. Proceedings of the 8th International Symposium on Water–Rock Interaction — WRI- 8, Vladivostok, Russia, 15-19 August 1995. A.A. Balkema, Rotterdam, pp. 79–82.

Fairchild, I. J., C. L. Smith, A. Baker, L. Fuller, C. Spotl, D. Mattey, and F. McDermott (2006), Modelling and preservation of enrivonmental environmental signals in speleothem. *Earth Science Review* 75, 105-153.

Ford, D. C., and P. W., Williams (1989), *Karst Geomorphology and Hydrology*. Chapman and Hall: London.

Frisia, S., A. Borsato, I. J. Fairchild, F. McDermott, E. M. Selmo (2002), Aragonite-Calcite Relationships in Speleothems (Grotte De Clamouse, France): Environment, Fabrics, and Carbonate Geochemistry. *Journal of Sedimentary Research*; September 2002; v. 72; no. 5; p. 687-699; DOI: 10.1306/020702720687.

Fernández-Cortés, A., J. M. Calaforra, F. Sánchez-Martos, and J. Gisbert (2007). Stalactite drip rate variations controlled by air pressure changes: an example of non‐linear infiltration processes in the 'Cueva del Agua'(Spain). *Hydrological processes* 21: 920-930.

493 Gran, G. (1952), Determination of equivalence point in potentiometric titration Part II.
494 *Analyst* 77, 661-671.
495 Harned, H. S., and S. R. Scholes (1941), The ionization constant of HCO− 3 from 0 to
496 50◦C, *J. Am. Chem. Soc.*, 63, 1706–1709.
497 Hendy, C. H. (1971), The isotopic geochemistry of speleothems- The calculation of the
498 effects of different modes of formation on the isotopic composition of
499 speleothems and their applicability as palaeoclimatic indicators. *Geochimica et*
500 *Cosmochimica Acta* 35, 801- 824.
501 Huang, H. M., and I. J. Fairchild (2001), Partitioning of Sr2+ and Mg2+ into calcite in
502 karst-analogue experimental solutions. *Geochimica et Cosmochimica Acta* 65:
503 47–62. DOI: 10.1016/S0016-7037(00)00513-5.
504 Huang, Y., I. J. Fairchild, A. Borsato, S. Frisia, N.J. Cassidy, F. McDermott, and C. J.
505 Hawkesworth (2001), Seasonal variations in Sr, Mg and P in modern speleothems
506 (Grotta di Ernesto, Italy). *Chemical Geology* 175:429–448.
507 Irwin, W.P. (1966), Geologic reconnaissance of the Northern Coast Ranges and Klamath
508 Mountains, California with a summary of mineral resources: California Division
509 of Mines and Geology Bulletin, v 179, 80p.
510 Johnson, K. R., C. Hu, N. S. Belshaw, and G. M. Henderson (2006), Seasonal trace
511 element and stable isotope variations in China speleothem: The potential for high
512 resolution paleo mansoon reconstruction. *Earth and Planetary Science Letter* 244,
513 394-407.

514 Karmann, I., F. W. Cruz Jr., O. Viana Jr., and S.J. Burns (2007), Climate influence on
515 geochemistry parameters of waters from Santana-Pérolas cave system, Brazil.
516 *Chemical Geology* 244, 232-247.
517 Lachniet, M. D. (2009), Climatic and environmental controls on speleothem oxygen-
518 isotope values. *Quat. Sci. Rev.* 28, 412-432.
519 Lahann, R. W. (1978a), A chemical model for calcite crystal growth and morphology
520 control. *J. Sed. Petrol.* 48, 337-341.
521 Lahann, R. W. (1978b), (Reply) A chemical model for calcite crystal growth and
522 morphology control. *J. Sed. Petrol.* 49, 337-341.
523 Lambert, W. J., and P. Aharon (2011), Controls on dissolved inorganic carbon and δ 13
524 C in cave waters from DeSoto Caverns: implications for speleothem δ13C
525 assessments. *Geochimica et Cosmochimica Acta,* 75(3), 753-768.
526 Land, L. S. (1967), Diagenesis of skeletal carbonate. *J. Sed. Petrol.* 37, 914-930.
527 Mackenzie, F. T., W. D. Bischoff, F. C. Bishop, M. Loijens, J. Schoonmaker, and R.
528 Wollast (1982), Magnesium calcite: Low-temperature occurrence, solubility and
529 solid solution behavior. In; Reed, R. J., (ed.) *Carbonate Mineralogy and*
530 *Chemistry Reviews in Mineralogy* 11, Ribbe, P. H., series (ed), p 97-144.
531 Mayer, J. (1999), Spatial and temporal variation of groundwater chemistry at Pettyjohns
532 Cave, northwest Georgia: *Journal of Cave and Karst Studies,* v. 61(3), p. 131-138.
533 McDonald, J., R. Drysdale, D. Hill (2004), El Nino recorded in Australian cave drip
534 waters: Implications for reconstructing rainfall histories using stalagmites.
535 *Geophysical Research Letters* 31, L22202, doi:10.1029/2004GL02859.

536 McDonald, J., R. Drysdale, D. Hill, R. Chisari, H. Wong (2007), The hydrochemical
537 response of cave drip waters to sub-annual and inter-annual climate variability,
538 Wombeyan caves, SE Australia, *Chemical Geology* 244, 605-623.
539 McDonald, M., and R. Drysdale (2007), Hydrology of cave drip waters at varying
540 bedrock depths from a karst system in southeastern Australia. *Hydrological*
541 *Process*. 21, 1737–1748. DOI: 10.1002/hyp.6356
542 McDermott, F. (2004), Palaeo-climate reconstruction from stable isotope variations in
543 speleothems: a review. *Quat. Sci. Rev*. 23(7-8), 901-918.
544 McMillan, E. A., I. J. Fairchild, S. Frisia, A. Borsato, F. McDermott (2005), Annual trace
545 element cycles in calcite–aragonite speleothems: evidence of drought in the
546 western Mediterranean 1200–1100 yr BP. *Journal of Quaternary Science* 20:423-
547 433. DOI: 10.1002/jqs.943
548 Mehrbach, C., C. H. Culberson, J. E. Hawley, and R. M. Pytkowicz (1973), Measurement
549 of the apparent dissociation constants of carbonic acid in seawater at atmospheric
550 pressure, *Limnol. Oceanogr.*, 18, 897–907.
551 Morse, J. W., and M. Bender (1990), Partition coefficients in calcite: examination of
552 factors influencing the validity of experimental results and their application to
553 natural systems. *Chem. Geol*. 82, 265-277.
554 Motyka, J., M. Gradziński, P. Bella, and P. Holúbek (2005), Chemistry of waters from
555 selected caves in Slovakia – a reconnaissance study: *Environmental Geology*, v.
556 48, p. 682-692, doi: 10.1007/s00254-005-000602.

557 Mucci, A., and J. W. Morse (1983), The incorporation of Mg2+ and Sr2+ into calcite
558 overgrowths: influences of growth rate and solution composition. *Geochimica et*
559 *Cosmochimica Acta* 47, 217-233.
560 Mucci, A., and J. M. Morse (1984), The solubility of calcite in seawater solutions at
561 various magnesian concentrations. It = 0.697m at 25oC and one atmospheric total
562 pressure. *Geochim. Cosmochim Acta*, 48, 815-822.
563 Mucci, A., J. M. Morse, and M. S. Kaminsky (1985), Auger spectroscopy analysis of
564 magnesium calcite overgrowth precipitated from seawater and solution of similar
565 composition. *Am. J. Sci.* 285, 289-305.
566 Musgrove, M., and J. L. Banner (2004), Controls on the spatial and temporal variability
567 of vados dripwater geochemistry; Edwards aquifer, central Texas. *Geochimica et*
568 *Cosmochimica Acta* 68; 1007-1020.
569 Parkhurst, D.L. (2007), U.S. Geological Survey;
570 http://wwwbrr.cr.usgs.gov/projects/GWC_coupled/phreeqci/index.html
571 Picknett, R. G., L. G. Bray, and R. D. Stenner (1976). The chemistry of cave water. In:
572 Ford, T. D. and C. H. C. Cullingford (ed.) *The Science of Speleology*. New York,
573 Academic Press, p. 213-266.
574 Plummer, L. N., and E. Busenberg (1982) The solubilities of calcite, aragonite and
575 vaterite in CO_2-H_2O solutions between 0 and 90°C and an evaluation of the
576 aqueous model for the system $CaCO_3$-CO_2-H_2O. *Geochim. Cosmochim. Acta* 46,
577 1011–1040.
578 Plummer, L. N., and F. T. Mckenzie (1974), Predicting mineral solubility from rate data:
579 Application to the dissolution of magnesian calcite. *Am. J. Sci.* 274, 61-83.

580 Pytkowicz, R. M., (1965), Rates of inorganic calcium carbonate nucleation. *J. Geol*. 3,
581 196-199.
582 Roth, J. E., (2005), Oregon Caves National Monument – Subsurface Management plan –
583 Environmental Assessment, National Park Service; U.S. Department of the
584 Interior.
585 Rushdi, A. I., (1995), Equilibrium behavior magnesian calcite mineral: A theoretical
586 approach. *J. K. A. U. Mar. Sci*., 6, 41-50.
587 Rushdi, A. I., C. T. A. Chen, and E. Suess (1998), Solubility of calcite in seawater
588 solution of different magnesium concentration at 25^{o}C and 1 Atm Pressure: A
589 laboratory re-examination. *La Mer*, 36, 9-22
590 Rushdi, A. I., R. M. Pytkowicz, E. Suess, and C. T. Chen (1992), The effect of
591 magnesium-to-calcium ratios in artificial seawater at different ionic products,
592 upon the induction time and mineralogy of calcium carbonate: a laboratory study.
593 *Geologisch Rundschan*, 81, 751-578.
594 Salinas, J., (2003), An Oregon caves water inventory: *Oregon Caves National Monument.*
595 *Report* CAS-0403.
596 Schubert, N. (2007), Study of a Karst Geochemical Data-Set from a Marble Cave:
597 Oregon Caves National Monument. University of Missouri, Columbia, 56pp.
598 Smart, P.L., H. Friederich, and S.T. Trudgill (1986), Controls on the composition of
599 authigenic percolation water in the Burren, Ireland. In: Paterson, K. and Sweeting,
600 M.M., Editors, 1986. Proceedings of the Anglo-French Karst Symposium, 1983
601 Proceedings of the Anglo-French Karst Symposium, 1983, pp. 17–47.

602 Steponaitis, E., Alexandra A., David M., Jay Q., Yu-Te ., Wallace S. B., Bryan N. S.,
603 Stephen J. B., and Hai C (2015). Mid-Holocene drying of the US Great Basin
604 recorded in Nevada speleothems. *Quaternary Science Reviews* 127: 174-185.
605 Taylor, G. C., and C. Hannan (1999), The Climate of Oregon: From Rainforest to Desert.
606 Oregon State University Press, Corvallis.
607 Thorstenson, D. D., and L. N. Plummer (1977), Equilibrium criteria for two component
608 solids reaction with fixed composition in an aqueous phase example: the
609 magnesian calcite. *Am. J. Sci*. 277, 1203-1223.
610 Tooth, A. F., and I. J. Fairchild (2003), Soil and karst aquifer hydrological controls on the
611 geochemical evolution of speleothem-forming drip waters, Crag Cave, southwest
612 Ireland. *Journal of Hydrology* 273 (2003) 51–68.
613 Toran, L., and E. Roman (2006), CO_2 outgasing in a combined fracture conduit karst
614 aquifer near Lititz Spring, Pennsylvania, in Harmon, R. S., and C. M. Wicks eds.,
615 Perspectives on karst geomorphology, hydrology, and geochemistry – A tribute
616 volume to Derek C. Ford and William B. White: Geological Society of America
617 Special Paper 404, p. 267-274, doi: 10.1130/2006.2404(22).
618 Vacco, D.A., Clark, P.U., Mix, A.C., Cheng, H. and Edwards, R.L., (2005). A
619 speleothem record of younger Dryas cooling, Klamath mountains, Oregon, USA.
620 *Quaternary Research*, *64*(2), pp.249-256.
621 Walter, L. M., and J. W. Morse (1984) Magnesian calcite stablilites: A reevaluation.
622 *Geochim. Cosmochim. Acta*. 48, 1059-1069.
623 Weyle, P. K., (1961), The carbonate saturatometer. *J. Geol*. 69, 32-44.

White, W. B. (1994), The anthodites from Skyline Caverns, Virginia: The Type locality. *Natl. Speleol. Soc. Bull*. 48: 20-26.

White, W. B. (2004), Palaeoclimate records from speleothems in limestone caves. In: Sasowsky, I. D., and J. Mylroie, (Eds.), *Studies of Cave Sediments. Physical and Chemical Records of Palaeoclimate*. Kluwer Academic, New York, pp. 135– 175.

Wu, K., Shen, L., Zhang, T., Xiao, Q., and Wang, A. (2015). Links between host rock, water, and speleothems of Xueyu Cave in Southwestern China: lithology, hydrochemistry, and carbonate geochemistry. *Arabian Journal of Geosciences*, *8*(11), 8999-9013.

Zeng, G., W. Luo, S, Wang, and X. Du (2015), Hydrogeochemical and climatic interpretations of isotopic signals from precipitation to drip waters in Liangfeng Cave, Guizhou Province, China. *Environ Earth Sci* 74, 1509-1519.

Table 1. Spearman correlation coefficient (r) of physicochemical parameters of drip-water samples from shallow (< 18m) and deep (> 20m) rooms at Oregon Caves National Monument from 2006-2007.

Shallow Rooms (KQR & IR)	**Drip**	**pH**	**TA**	**Ba2+**	**Ca2+**	**Mg2+**	**Na+**	**Sr2+**
Drip	**1**	**-0.014**	**-.402***	**0.126**	**-.370***	**-0.121**	**-0.214**	**-0.061**
pH		**1**	**-0.058**	**.409***	**-0.258**	**-0.035**	**-0.14**	**0.063**
TA			**1**	**-.362***	**.924****	**0.271**	**0.007**	**0.183**
Ba2+				**1**	**-.407***	**.351***	**0.157**	**.439***
Ca2+					**1**	**0.252**	**0.093**	**0.151**
Mg2+						**1**	**0.175**	**.940****
Na+							**1**	**0.136**
Sr2+								**1**
Mg/Ca								
Sr/Ca								
Ba/Ca								
Na/Ca								
Deep Rooms (MR & SR1+2)								
Drip	**1**	**.546****	**-.313***	**0.21**	**-0.202**	**.356***	**-.281***	**-.287***
pH		**1**	**-0.253**	**.293***	**-0.177**	**-0.015**	**-0.162**	**-.387****
TA			**1**	**-0.273**	**.818****	**0.086**	**-0.028**	**.431***
Ba2+				**1**	**-.454***	**-0.018**	**0.035**	**0.052**
Ca2+					**1**	**0.188**	**-0.034**	**.396***
Mg2+						**1**	**0.13**	**.600****
Na+							**1**	**0.251**
Sr2+								**1**
Mg/Ca								
Sr/Ca								
Ba/Ca								

Na/Ca

**. Correlation is significant at the 0.01 level (2-tailed); * Correlation is significant at the 0.05 level (2-tailed).

Table 2. Principal component (PC) factors to physicochemical parameters of dripwaters from all cave sites.

	All	
	PC1	PC2
Dripping	0.701	-0.229
pH	0.976	-0.198
TA	-0.944	0.323
Ba2+	0.974	0.089
Ca2+	-0.923	0.345
Mg2+	0.947	-0.294
Na+	0.757	-0.605
Sr2+	-0.119	0.98
Eigen value	6.29	1.068
Total variance (%)	78.62	13.34
Cumulative (%)	78.62	91.96

Table 4. Carbonate chemical parameters of dripwater solutions from Oregon Caves National Monument Cave.

	Site				
	IR	**KQR**	**MR**	**SR1**	**SR2**
Sampling Period	Jan 05-Apr 07	Dec 05-May 07	Dec 06-May07	Jan-Jul 2007	Dec 06-Jul 08
CA (meq L^{-1})					
Minimum	2.1015	2.1408	1.9989	2.0778	2.1314
Maximum	2.9200	2.8134	2.6539	2.3812	2.3316
Mean (Standard Deviation)	2.4710 (0.2200)	2.4407 (0.0616)	2.2997 (0.0444)	2.2047 (0.0228)	2.1891 (0.0611)
TCO_2 (mole L^{-1})					
Minimum	2.1459	2.1637	2.0197	2.0806	2.1245
Maximum	2.9657	2.8266	2.6620	2.4434	2.3701
Mean (Standard Deviation)	2.5043 (0.2231)	2.4683 (0.0633)	2.3165 (0.0431)	2.2220 (0.0285)	2.2030 (0.0777)
%Ω (Calcite)					
Minimum	86	151	156	139	131
Maximum	528	462	472	375	396
Mean (Standard Deviation)	262 (110)	267 (22)	277 (20)	279 (25)	284 (85)
%Ω (Aragonite)					
Minimum	59	105	108	97	91
Maximum	368	322	328	261	275
Mean (Standard Deviation)	182 (77)	186 (15)	193 (14)	194 (17)	197 (59)
%Ω (Vaterite)					
Minimum	21	36	38	34	32
Maximum	128	112	114	91	96
Mean (Standard Deviation)	63 (26)	64 (5)	67 (5)	67 (6)	69 (21)

Figure Captions

Figure 1. Map showing the locations of (a) Oregon Caves National Monument (OCNM), which is located in the Klamath Mountains, western the United States of America and (b) the water sampling sites in the OCNM caves.

Figure 2. Monthly variations of: (a) Rainfall, (b) dripwater rate, (c) pH, (d) total alkalinity (TA), (e) calcium (Ca^{2+}), (f) magnesium (Mg^{2+}), (g) strontium (Sr^{2+}) and (h) barium (Ba^{2+}) in dripwaters during monitoring program from January 2005 to April 2007.

Figure 3. Plot showing: (a) the dendrogram of cluster analysis (CA) and (b) the principal component analysis (PCA) for the physicochemical parameters.

Figure 4. Plots of Carbonate alkalinity (CA) vs. calcium (Ca^{2+}) for dripwaters of all sites.

Figure 5. Percent saturations of the drip waters with respect to: (a) calcite, (b) arabonite and (c) varetrite.

Figure 6. Plots of the variation trends and relationships between different parameters in dripwaters of the different rooms as a result of dissolution and reprecipitation reactions: (a) Ca vs. Ω%, (b) Sr/Ca vs Mg/Ca ratios, (c) Ω% vs. Mg/Ca ratios, (d) Ω% vs. Sr/Ca ratios, (e) Ca vs. Mg/Ca ratio, and (f) Ca vs. Sr/Ca ratio for all sites.

F1

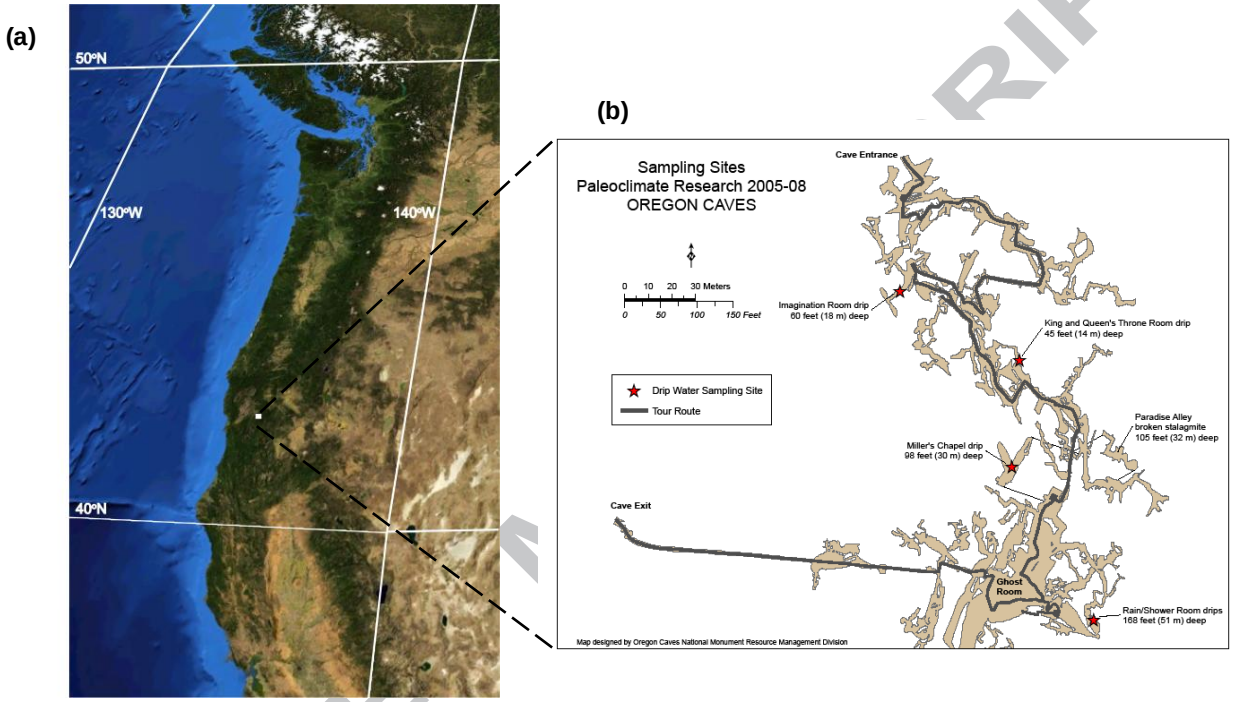

F2

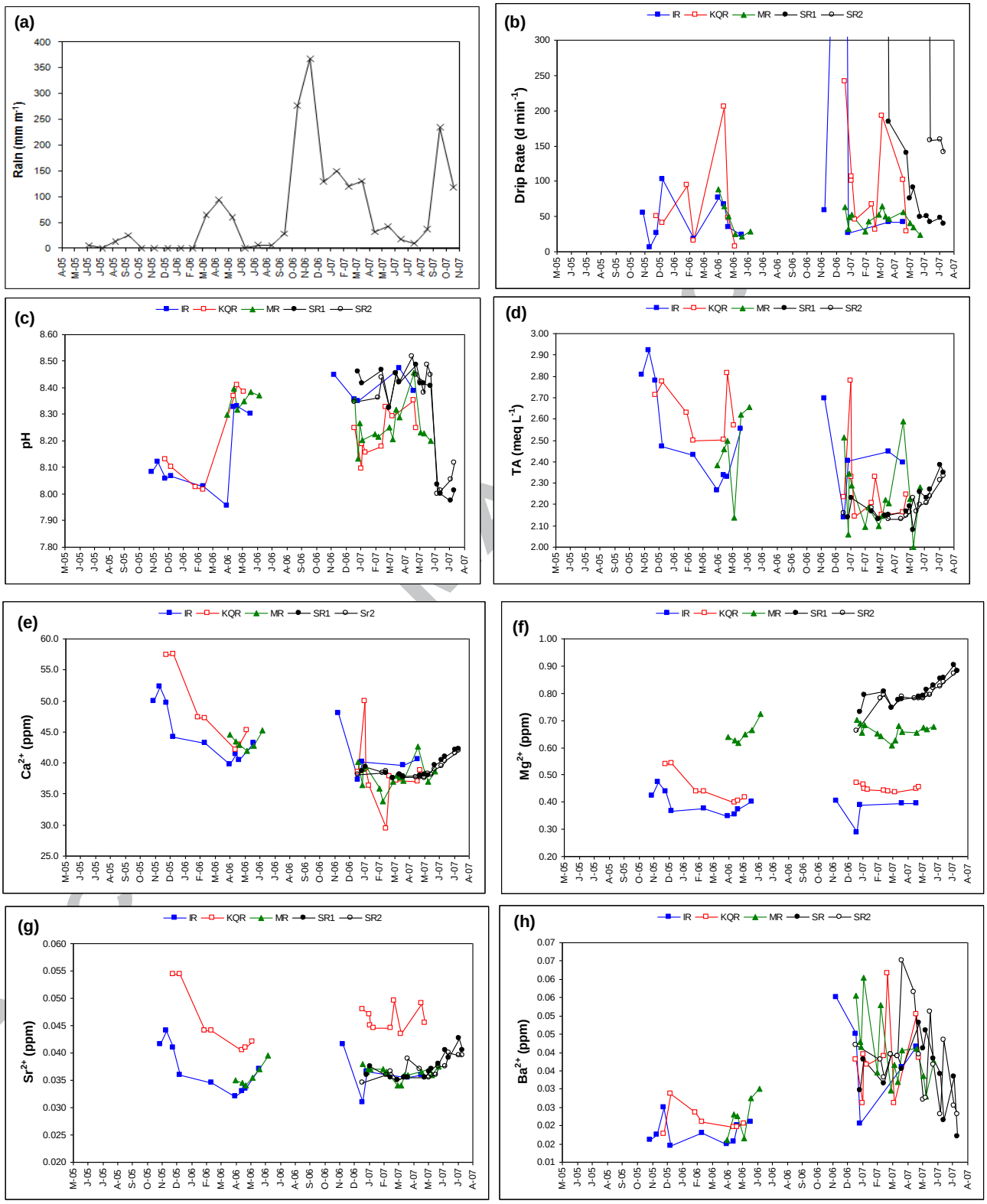

F3

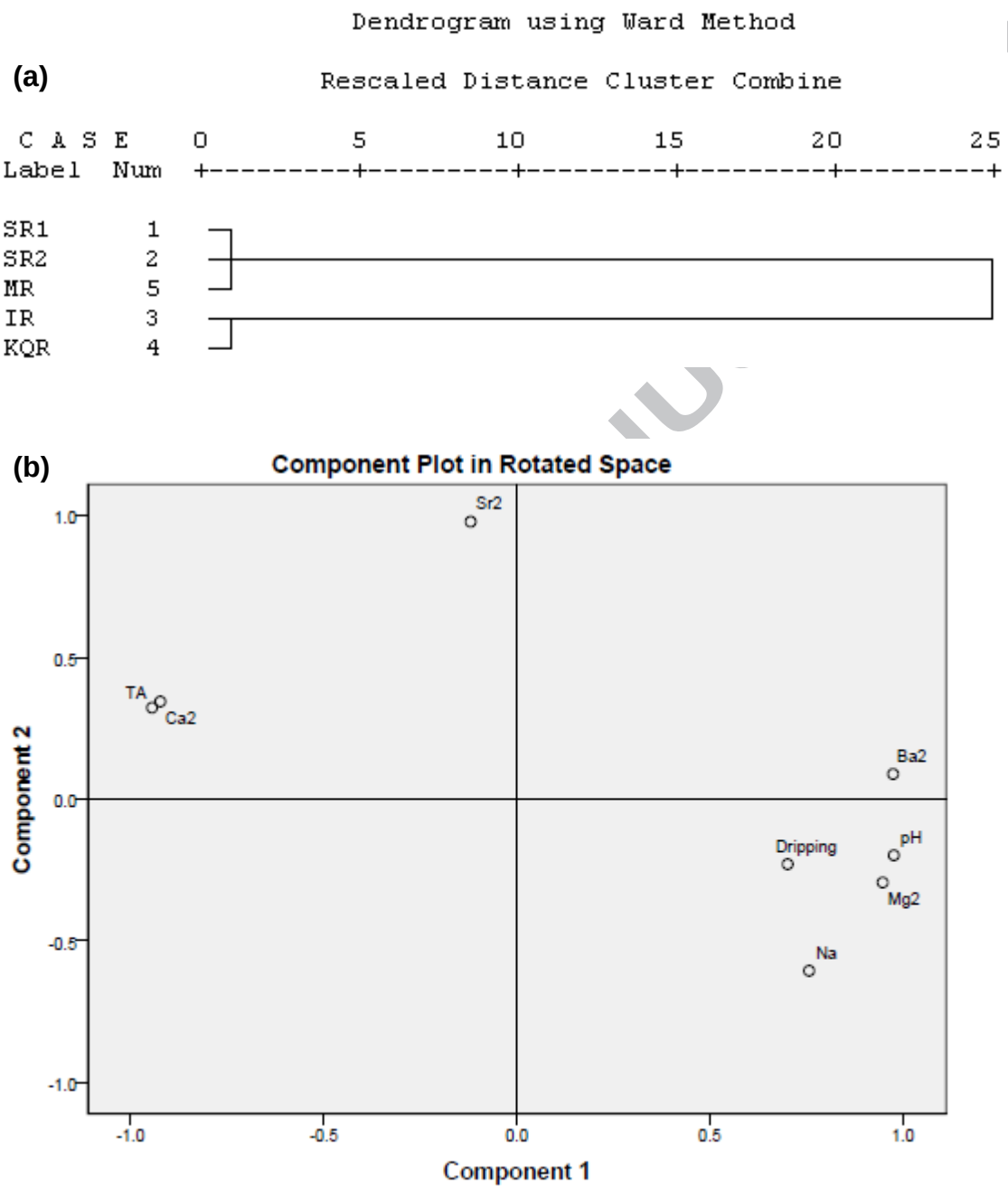

F4

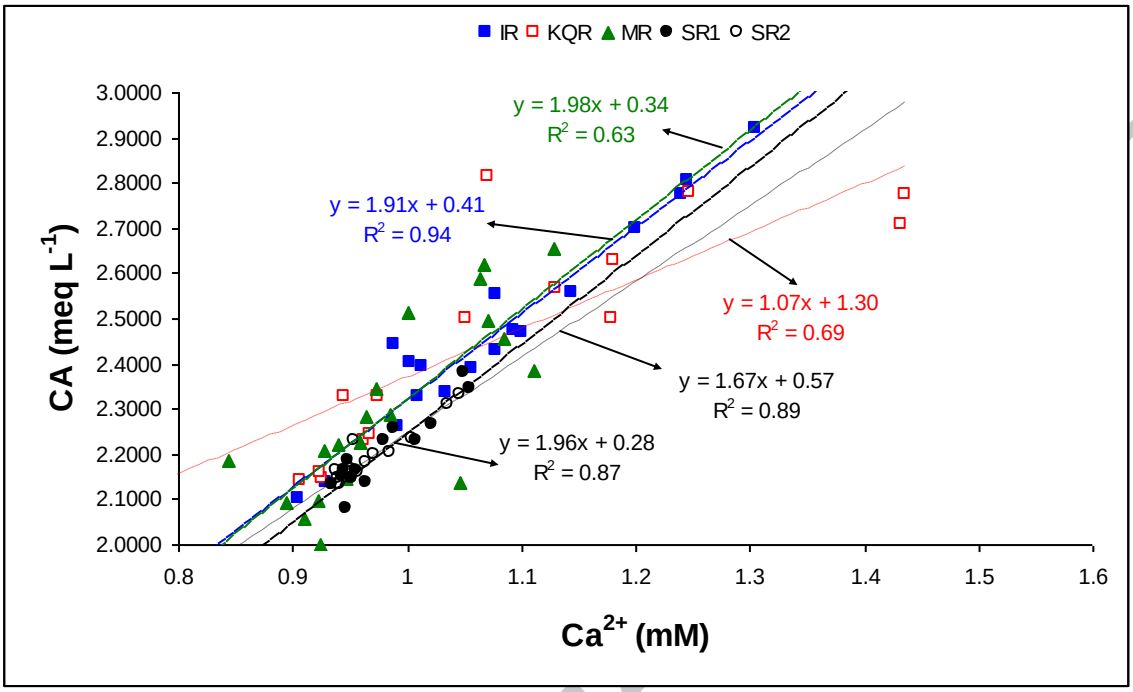

F5

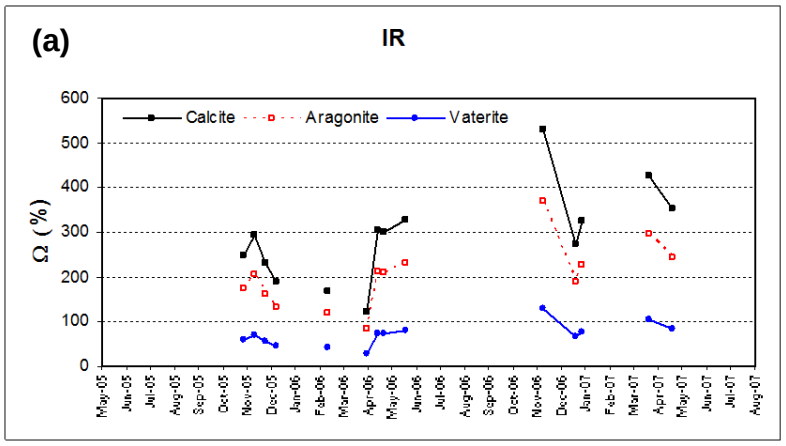

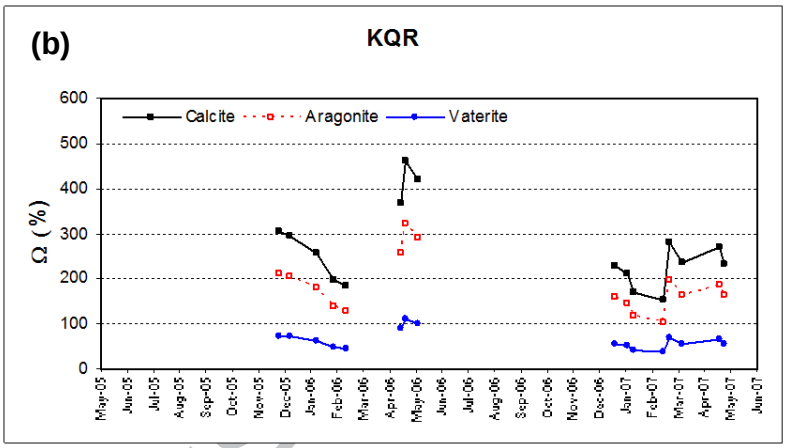

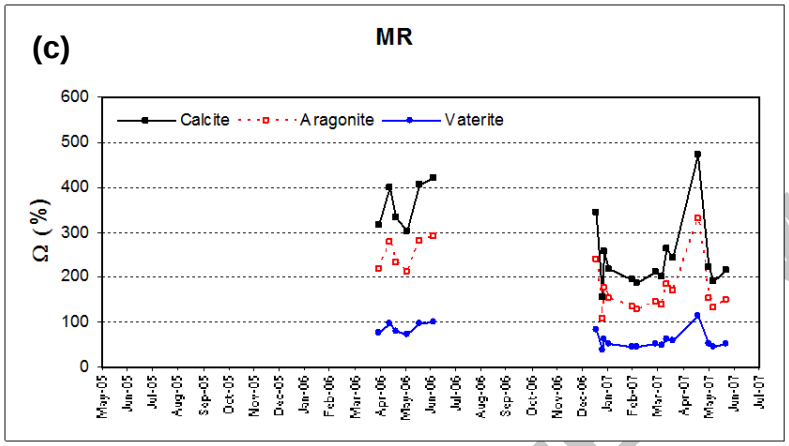

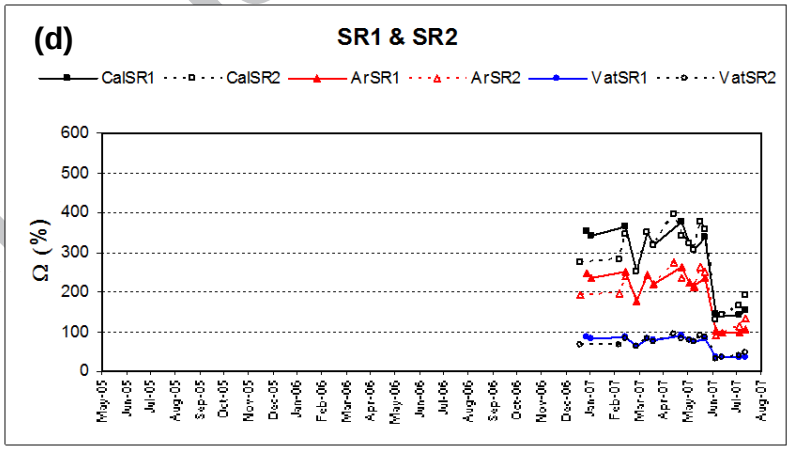

Fig 6

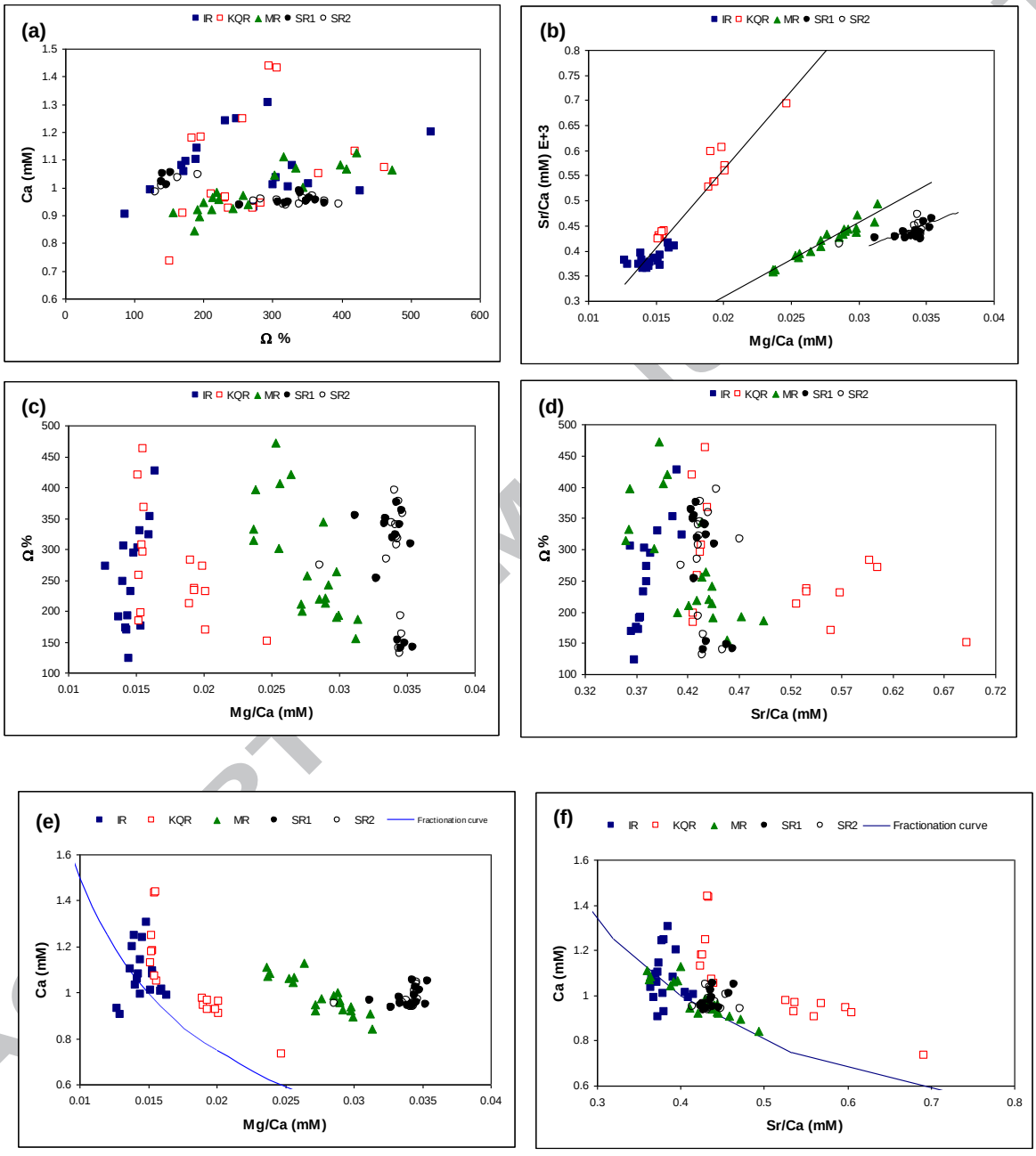

Highlights

- Cave dripwater chemistry of Oregon Caves National Monument (OCNM) was studied.
- The dripwater varies in response to seasonal changes in rainfall.
- Spatial variations of dripwater chemistry reflect the chemical composition of bedrock
- The residence time of infiltrated water in bedrock cracks control the dissolution and reprecipitation of calcium carbonate.
- Dripwater Mg/Ca and Sr/Ca ratios are controlled by dissolution and reprecipitation of carbonate bedrock.